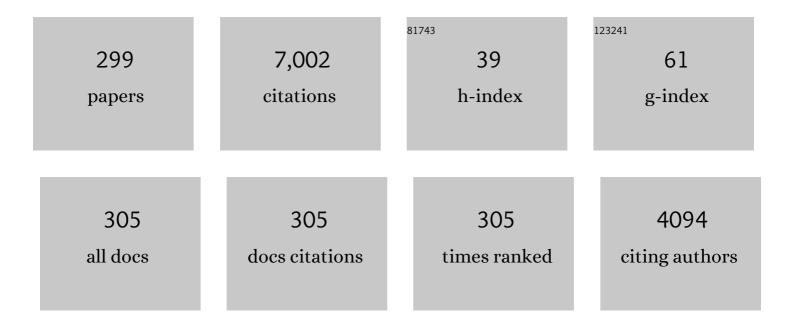
List of Publications by Year in descending order

Source: https://exaly.com/author-pdf/8502336/publications.pdf

Version: 2024-02-01



WALTER LOSÃO BOTTA

#	Article	IF	CITATIONS
1	Excess free volume in metallic glasses measured by X-ray diffraction. Acta Materialia, 2005, 53, 1611-1619.	3.8	344
2	Nanomaterials by severe plastic deformation: review of historical developments and recent advances. Materials Research Letters, 2022, 10, 163-256.	4.1	215
3	Improvement in H-sorption kinetics of MgH powders by using Fe nanoparticles generated by reactive FeF addition. Scripta Materialia, 2005, 52, 719-724.	2.6	174
4	Shear delocalization and crack blunting of a metallic glass containing nanoparticles: In situ deformation in TEM analysis. Scripta Materialia, 2006, 54, 1829-1834.	2.6	112
5	Hydrogen-induced phase transition of MgZrTiFe0.5Co0.5Ni0.5 high entropy alloy. International Journal of Hydrogen Energy, 2018, 43, 1702-1708.	3.8	111
6	An investigation of hydrogen storage in a magnesium-based alloy processed by equal-channel angular pressing. International Journal of Hydrogen Energy, 2013, 38, 8306-8312.	3.8	96
7	Microstructure and wear behavior of Fe-based amorphous HVOF coatings produced from commercial precursors. Surface and Coatings Technology, 2017, 309, 938-944.	2.2	92
8	Corrosion resistance of Fe-based amorphous alloys. Journal of Alloys and Compounds, 2014, 586, S105-S110.	2.8	90
9	High Strength AA7050 Al alloy processed by ECAP: Microstructure and mechanical properties. Materials Science & Engineering A: Structural Materials: Properties, Microstructure and Processing, 2011, 528, 5804-5811.	2.6	89
10	Nanoscale Grain Refinement and Hâ€5orption Properties of MgH <sub>2</sub> Processed by Highâ€Pressure Torsion and Other Mechanical Routes. Advanced Engineering Materials, 2010, 12, 786-792.	1.6	82
11	Influence of processing parameters on the fabrication of a Cu-Al-Ni-Mn shape-memory alloy by selective laser melting. Additive Manufacturing, 2016, 11, 23-31.	1.7	80
12	Structural characterization and dehydrogenation behavior of Mg–5 at.%Nb nano-composite processed by reactive milling. Journal of Alloys and Compounds, 2004, 376, 251-256.	2.8	77
13	Plasticity induced by nanoparticle dispersions in bulk metallic glasses. Journal of Non-Crystalline Solids, 2007, 353, 327-331.	1.5	76
14	H-sorption in MgH2 nanocomposites containing Fe or Ni with fluorine. Journal of Alloys and Compounds, 2005, 404-406, 409-412.	2.8	73
15	Topological instability as a criterion for design and selection of aluminum-based glass-former alloys. Applied Physics Letters, 2005, 86, 211904.	1.5	72
16	Synthesis and hydrogen storage behavior of Mg–V–Al–Cr–Ni high entropy alloys. International Journal of Hydrogen Energy, 2021, 46, 2351-2361.	3.8	69
17	Microstructure evolution and mechanical properties of Al–Zn–Mg–Cu alloy reprocessed by spray-forming and heat treated at peak aged condition. Journal of Alloys and Compounds, 2013, 579, 169-173.	2.8	67
18	Mechanical activation of TiFe for hydrogen storage by cold rolling under inert atmosphere. International Journal of Hydrogen Energy, 2018, 43, 2913-2918.	3.8	66

#	Article	IF	CITATIONS
19	Correlation between hydrogen storage properties and textures induced in magnesium through ECAP and cold rolling. International Journal of Hydrogen Energy, 2014, 39, 3810-3821.	3.8	63
20	Mg alloy for hydrogen storage processed by SPD. International Journal of Materials Research, 2009, 100, 1739-1746.	0.1	62
21	Improving H-sorption in MgH2 powders by addition of nanoparticles of transition metal fluoride catalysts and mechanical alloying. Journal of Alloys and Compounds, 2005, 389, 270-274.	2.8	60
22	lron and niobium based additives in magnesium hydride: Microstructure and hydrogen storage properties. International Journal of Hydrogen Energy, 2017, 42, 6810-6819.	3.8	57
23	Formation of Fe-based glassy matrix composite coatings by laser processing. Surface and Coatings Technology, 2014, 240, 336-343.	2.2	56
24	Microstructure evolution in copper under severe plastic deformation detected by in situ X-ray diffraction using monochromatic synchrotron light. Materials Science & Engineering A: Structural Materials: Properties, Microstructure and Processing, 2009, 503, 10-13.	2.6	54
25	Nanostructured MgH2 prepared by cold rolling and cold forging. Journal of Alloys and Compounds, 2011, 509, S444-S448.	2.8	54
26	Corrosion properties of Fe–Cr–Nb–B amorphous alloys and coatings. Surface and Coatings Technology, 2014, 254, 238-243.	2.2	53
27	Consolidation of partially amorphous aluminium-alloy powders by severe plastic deformation. Materials Science & Engineering A: Structural Materials: Properties, Microstructure and Processing, 2004, 375-377, 936-941.	2.6	50
28	Nanostructured composites obtained by reactive milling. Scripta Materialia, 2001, 44, 1735-1740.	2.6	49
29	Magnetic properties evaluation of spray formed and rolled Fe–6.5wt.% Si–1.0wt.% Al alloy. Materials Science & Engineering A: Structural Materials: Properties, Microstructure and Processing, 2007, 449-451, 375-377.	2.6	48
30	Magnetic properties of spray-formed Fe–6.5%Si and Fe–6.5%Si–1.0%Al after rolling and heat treatment. Journal of Magnetism and Magnetic Materials, 2008, 320, e653-e656.	1.0	48
31	Partial crystallization and corrosion resistance of amorphous Fe-Cr-M-B (M=Mo, Nb) alloys. Journal of Non-Crystalline Solids, 2010, 356, 2651-2657.	1.5	44
32	Effects of equal-channel angular pressing and accumulative roll-bonding on hydrogen storage properties of a commercial ZK60 magnesium alloy. International Journal of Hydrogen Energy, 2015, 40, 16971-16976.	3.8	44
33	Sliding wear of spray-formed high-chromium white cast iron alloys. Wear, 2005, 259, 445-452.	1.5	42
34	Formation, stability and ultrahigh strength of novel nanostructured alloys by partial crystallization of high-entropy (Fe0.25Co0.25Ni0.25Cr0.125Mo0.125)86‒89B11‒14 amorphous phase. Acta Materialia, 20 170, 50-61.	193.8	42
35	Corrosion and wear properties of FeCrMnCoSi HVOF coatings. Surface and Coatings Technology, 2019, 357, 993-1003.	2.2	42
36	Effect of boron addition on the solidification sequence and microstructure of AlCoCrFeNi alloys. Journal of Alloys and Compounds, 2019, 775, 1235-1243.	2.8	42

#	Article	IF	CITATIONS
37	Laser surface remelting of a Cu-Al-Ni-Mn shape memory alloy. Materials Science & Engineering A: Structural Materials: Properties, Microstructure and Processing, 2016, 661, 61-67.	2.6	41
38	Mg-Zn-Ca amorphous alloys for application as temporary implant: Effect of Zn content on the mechanical and corrosion properties. Materials and Design, 2016, 110, 188-195.	3.3	41
39	Microstructure and mechanical properties of spray deposited hypoeutectic Al–Si alloy. Materials Science & Engineering A: Structural Materials: Properties, Microstructure and Processing, 2004, 375-377, 577-580.	2.6	40
40	Hydrogen storage properties of pure Mg after the combined processes of ECAP and cold-rolling. Journal of Alloys and Compounds, 2014, 586, S405-S408.	2.8	40
41	Degradation of biodegradable implants: The influence of microstructure and composition of Mg-Zn-Ca alloys. Journal of Alloys and Compounds, 2019, 774, 168-181.	2.8	40
42	An approach to design single BCC Mg-containing high entropy alloys for hydrogen storage applications. International Journal of Hydrogen Energy, 2021, 46, 25555-25561.	3.8	40
43	Mg-containing multi-principal element alloys for hydrogen storage: A study of the MgTiNbCr0.5Mn0.5Ni0.5 and Mg0.68TiNbNi0.55 compositions. International Journal of Hydrogen Energy, 2020, 45, 19539-19552.	3.8	39
44	Reaction sintering of titanium carbide and titanium silicide prepared by high-energy milling. Materials Science & Engineering A: Structural Materials: Properties, Microstructure and Processing, 2002, 336, 202-208.	2.6	38
45	Gene expression of human osteoblasts cells on chemically treated surfaces of Ti–6Al–4V–ELI. Materials Science and Engineering C, 2015, 51, 248-255.	3.8	38
46	Wear resistant coatings of boron-modified stainless steels deposited by Plasma Transferred Arc. Surface and Coatings Technology, 2016, 302, 255-264.	2.2	38
47	Metastable phases in Zr-based bulk glass-forming alloys detected using a synchrotron beam in transmission. Materials Science & Engineering A: Structural Materials: Properties, Microstructure and Processing, 2001, 304-306, 34-38.	2.6	37
48	Glass forming ability of the Al–Ce–Ni system. Journal of Non-Crystalline Solids, 2008, 354, 4874-4877.	1.5	37
49	Cold rolling of MgH2 powders containing different additives. International Journal of Hydrogen Energy, 2013, 38, 16193-16198.	3.8	37
50	Design of TiVNb-(Cr, Ni or Co) multicomponent alloys with the same valence electron concentration for hydrogen storage. Journal of Alloys and Compounds, 2021, 865, 158767.	2.8	37
51	Topological instability and electronegativity effects on the glass-forming ability of metallic alloys. Philosophical Magazine Letters, 2008, 88, 785-791.	0.5	36
52	Phase Formation, Thermal Stability and Mechanical Properties of a Cu-Al-Ni-Mn Shape Memory Alloy Prepared by Selective Laser Melting. Materials Research, 2015, 18, 35-38.	0.6	36
53	Microstructural investigation of Fe Cr Nb B amorphous/nanocrystalline coating produced by HVOF. Materials and Design, 2016, 111, 608-615.	3.3	36
54	Corrosion properties of amorphous, partially, and fully crystallized Fe68Cr8Mo4Nb4B16 alloy. Journal of Alloys and Compounds, 2020, 826, 154123.	2.8	36

WALTER JOSé BOTTA

#	Article	IF	CITATIONS
55	Amorphous phase formation in spray deposited AlYNiCo and AlYNiCoZr alloys. Scripta Materialia, 2001, 44, 1625-1628.	2.6	35
56	Al2O3–WC synthesis by high-energy reactive milling. Materials Science & Engineering A: Structural Materials: Properties, Microstructure and Processing, 2007, 464, 47-51.	2.6	35
57	Osteoblasts behavior on chemically treated commercially pure titanium surfaces. Journal of Biomedical Materials Research - Part A, 2014, 102, 1816-1822.	2.1	35
58	Reassessment of the effects of Ce on quasicrystal formation and microstructural evolution in rapidly solidified Al–Mn alloys. Acta Materialia, 2015, 98, 221-228.	3.8	35
59	Design of wear resistant boron-modified supermartensitic stainless steel by spray forming process. Materials and Design, 2015, 83, 214-223.	3.3	35
60	Reduced electronegativity difference as a factor leading to the formation of Al-based glassy alloys with a large supercooled liquid region of 50K. Applied Physics Letters, 2006, 88, 011911.	1.5	34
61	Crystallisation behaviours of Al-based metallic glasses: Compositional and topological aspects. Journal of Alloys and Compounds, 2009, 483, 89-93.	2.8	34
62	Homogenization of plastic deformation in metallic glass foils less than one micrometer thick. Physical Review B, 2010, 82, .	1.1	34
63	Spray forming of Cu–11.85Al–3.2Ni–3Mn (wt%) shape memory alloy. Journal of Alloys and Compounds, 2014, 615, S602-S606.	2.8	34
64	Crystallization behavior of amorphous Al84Y9Ni5Co2 alloy. Materials Science & Engineering A: Structural Materials: Properties, Microstructure and Processing, 2001, 304-306, 332-337.	2.6	33
65	Atomization and Selective Laser Melting of a Cu-Al-Ni-Mn Shape Memory Alloy. Materials Science Forum, 0, 802, 343-348.	0.3	33
66	Challenges in optimizing the resistance to corrosion and wear of amorphous Fe-Cr-Nb-B alloy containing crystalline phases. Journal of Non-Crystalline Solids, 2021, 555, 120537.	1.5	33
67	Room temperature hydrogen absorption by Mg andÂMg TiFe nanocomposites processed by high-energy ball milling. International Journal of Hydrogen Energy, 2018, 43, 12251-12259.	3.8	32
68	Hydrogen Storage in Mg and Mg-Based Alloys and Composites Processed by Severe Plastic Deformation. Materials Transactions, 2019, 60, 1561-1570.	0.4	32
69	Electrochemical impedance analysis of TiO2 nanotube porous layers based on an alternative representation of impedance data. Journal of Electroanalytical Chemistry, 2015, 737, 54-64.	1.9	31
70	Surface anodization of the biphasic Ti13Nb13Zr biocompatible alloy: Influence of phases on the formation of TiO2 nanostructures. Journal of Alloys and Compounds, 2019, 796, 93-102.	2.8	31
71	Recent developments on fabrication of Alâ€matrix composites reinforced with quasicrystals: From metastable to conventional processing. Journal of Materials Research, 2021, 36, 281-297.	1.2	31
72	Corrosion resistance of WE43 Mg alloy in sodium chloride solution. Materials Chemistry and Physics, 2021, 272, 124930.	2.0	31

#	Article	IF	CITATIONS
73	Amorphous phase formation during spray forming of Al84Y3Ni8Co4Zr1 alloy. Journal of Non-Crystalline Solids, 2001, 284, 134-138.	1.5	30
74	Cold rolling under inert atmosphere: A powerful tool for Mg activation. International Journal of Hydrogen Energy, 2014, 39, 4959-4965.	3.8	30
75	Topological Instability as a Criterion for Design and Selection of Easy Glass-Former Compositions in Cu-Zr Based Systems. Materials Transactions, 2007, 48, 1739-1742.	0.4	29
76	Thermodynamic analysis of the effect of annealing on the thermal stability of a Cu–Al–Ni–Mn shape memory alloy. Thermochimica Acta, 2015, 608, 1-6.	1.2	29
77	Evolution of the texture of spray-formed Fe–6.5wt.% Si–1.0wt.% Al alloy during warm-rolling. Materials Science & Engineering A: Structural Materials: Properties, Microstructure and Processing, 2007, 449-451, 854-857.	2.6	28
78	Microstructural characterization of a laser remelted coating of Al91Fe4Cr3Ti2 quasicrystalline alloy. Scripta Materialia, 2009, 61, 709-712.	2.6	28
79	Production and Corrosion Resistance of Thermally Sprayed Fe-Based Amorphous Coatings from Mechanically Milled Feedstock Powders. Metallurgical and Materials Transactions A: Physical Metallurgy and Materials Science, 2018, 49, 4860-4870.	1.1	28
80	Thermodynamic modelling of hydrogen-multicomponent alloy systems: Calculating pressure-composition-temperature diagrams. Acta Materialia, 2021, 215, 117070.	3.8	28
81	Crystallization of Fe-based amorphous alloys. Journal of Non-Crystalline Solids, 1999, 247, 19-25.	1.5	27
82	Microstructure and wear resistance of spray formed high chromium white cast iron. Materials Science & Engineering A: Structural Materials: Properties, Microstructure and Processing, 2004, 375-377, 589-594.	2.6	27
83	Processing of Al matrix composites reinforced with Al–Ni compounds and Al2O3 by reactive milling and reactive sintering. Journal of Alloys and Compounds, 2009, 471, 448-452.	2.8	27
84	H-sorption properties and structural evolution of Mg processed by severe plastic deformation. Journal of Alloys and Compounds, 2013, 580, S187-S191.	2.8	27
85	Enhancement of Mechanical Properties of Aluminum and 2124 Aluminum Alloy by the Addition of Quasicrystalline Phases. Materials Research, 2016, 19, 74-79.	0.6	27
86	Phase transformation and shape memory effect of a Cu-Al-Ni-Mn-Nb high temperature shape memory alloy. Materials Science & Engineering A: Structural Materials: Properties, Microstructure and Processing, 2016, 663, 64-68.	2.6	27
87	Structural, mechanical and thermal characterization of an Al-Co-Fe-Cr alloy for wear and thermal barrier coating applications. Surface and Coatings Technology, 2017, 319, 241-248.	2.2	27
88	Effect of cold rolling on the structure and hydrogen properties of AZ91 and AM60D magnesium alloys processed by ECAP. International Journal of Hydrogen Energy, 2017, 42, 21822-21831.	3.8	27
89	Synthesis and hydrogen sorption properties of Mg2FeH6–MgH2 nanocomposite prepared by reactive milling. Journal of Alloys and Compounds, 2012, 536, S250-S254.	2.8	26
90	An alternative route to produce easily activated nanocrystalline TiFe powder. International Journal of Hydrogen Energy, 2018, 43, 16107-16116.	3.8	26

#	Article	IF	CITATIONS
91	Fabrication of Al-matrix composite reinforced with quasicrystals using conventional metallurgical fabrication methods. Scripta Materialia, 2019, 173, 21-25.	2.6	26
92	In situ crystallization of Zr55Cu30Al10Ni5 bulk glass forming from the glassy and undercooled liquid states using synchrotron radiation. Journal of Non-Crystalline Solids, 1999, 247, 31-34.	1.5	25
93	Phases formed during crystallization of Zr55Al10Ni5Cu30 metallic glass containing oxygen. Journal of Non-Crystalline Solids, 2002, 304, 51-55.	1.5	25
94	Topological instability, average electronegativity difference and glass forming ability of amorphous alloys. Intermetallics, 2009, 17, 183-185.	1.8	25
95	Microstructure study of Al 7050 alloy reprocessed by spray forming and hot-extrusion and aged at 121°C. Intermetallics, 2013, 43, 182-187.	1.8	25
96	MgH2Â+ÂFeNb nanocomposites for hydrogen storage. Materials Chemistry and Physics, 2014, 147, 557-562.	2.0	25
97	Severely deformed ZK60Â+Â2.5% Mm alloy for hydrogen storage produced by two different processing routes. International Journal of Hydrogen Energy, 2016, 41, 11284-11292.	3.8	25
98	Hydrogen storage in MgH2LaNi5 composites prepared by cold rolling under inert atmosphere. International Journal of Hydrogen Energy, 2018, 43, 13348-13355.	3.8	25
99	Unusual room temperature ductility of glassy copper–zirconium caused by nanoparticle dispersions that grow during shear. Materials Science & Engineering A: Structural Materials: Properties, Microstructure and Processing, 2007, 449-451, 105-110.	2.6	24
100	Nanoquasicrystalline Al–Fe–Cr–Nb alloys produced by powder metallurgy. Journal of Alloys and Compounds, 2013, 577, 650-657.	2.8	24
101	Processing and characterization of amorphous magnesium based alloy for application in biomedical implants. Journal of Materials Research and Technology, 2014, 3, 203-209.	2.6	24
102	Wear and corrosion properties of HVOF coatings from Superduplex alloy modified with addition of boron. Surface and Coatings Technology, 2017, 309, 911-919.	2.2	24
103	The formation of quasicrystals in Al-Cu-Fe-(M=Cr,Ni) melt-spun ribbons. Journal of Alloys and Compounds, 2018, 731, 1288-1294.	2.8	24
104	Single step fabrication by spray forming of large volume Al-based composites reinforced with quasicrystals. Scripta Materialia, 2020, 181, 86-91.	2.6	24
105	Effects of the Chromium Content in (TiVNb)100â^'xCrx Body-Centered Cubic High Entropy Alloys Designed for Hydrogen Storage Applications. Energies, 2021, 14, 3068.	1.6	24
106	Spray forming of glass former Fe63Nb10Al4Si3B20 alloy. Materials Science & Engineering A: Structural Materials: Properties, Microstructure and Processing, 2007, 449-451, 884-889.	2.6	23
107	Severe plastic deformation of Mg-Fe powders to produce bulk hydrides. Journal of Physics: Conference Series, 2009, 144, 012015.	0.3	23
108	MgH2-based nanocomposites prepared by short-time high energy ball milling followed byÂcold rolling: A new processing route. International Journal of Hydrogen Energy, 2014, 39, 4404-4413.	3.8	23

#	Article	IF	CITATIONS
109	Hydrogen storage in heavily deformed ZK60 alloy modified with 2.5Âwt.% Mm addition. International Journal of Hydrogen Energy, 2016, 41, 4177-4184.	3.8	23
110	Anelastic behaviour in Nbî—,Ti alloys containing interstitial elements. Journal of Alloys and Compounds, 1994, 211-212, 37-40.	2.8	22
111	Application of mathematical simulation and the factorial design method to the optimization of the atomization stage in the spray forming of a Cu–6% Zn alloy. Journal of Materials Processing Technology, 2000, 102, 221-229.	3.1	22
112	Processing of aluminium alloys containing titanium addition by mechanical alloying. Materials Science & Engineering A: Structural Materials: Properties, Microstructure and Processing, 2004, 375-377, 1201-1205.	2.6	22
113	The formation of quasicrystal phase in Al-Cu-Fe system by mechanical alloying. Materials Research, 2012, 15, 749-752.	0.6	22
114	Wear-resistant boride reinforced steel coatings produced by non-vacuum electron beam cladding. Surface and Coatings Technology, 2020, 386, 125466.	2.2	22
115	Characterization of hydrogen storage properties of Mg-Fe-CNT composites prepared by ball milling, hot-extrusion and severe plastic deformation methods. International Journal of Hydrogen Energy, 2016, 41, 23092-23098.	3.8	21
116	Fast hydrogen absorption/desorption kinetics in reactive milled Mg-8 mol% Fe nanocomposites. International Journal of Hydrogen Energy, 2020, 45, 12408-12418.	3.8	21
117	Interaction between Fe66Cr10Nb5B19 metallic glass and aluminum during spark plasma sintering. Materials Science & Engineering A: Structural Materials: Properties, Microstructure and Processing, 2021, 799, 140165.	2.6	21
118	Metallurgical processing of Mg alloys and MgH2 for hydrogen storage. Journal of Alloys and Compounds, 2022, 897, 162798.	2.8	21
119	Amorphous phase formation in Fe-6.0wt%Si alloy by mechanical alloying. Scripta Materialia, 1999, 42, 213-217.	2.6	20
120	Amorphous and nanostructured Al–Fe–Nd powders obtained by gas atomization. Materials Science & Engineering A: Structural Materials: Properties, Microstructure and Processing, 2001, 315, 89-97.	2.6	20
121	Severe plastic deformation and different surface treatments on the biocompatible Ti13Nb13Zr and Ti35Nb7Zr5Ta alloys: Microstructural and phase evolutions, mechanical properties, and bioactivity analysis. Journal of Alloys and Compounds, 2020, 812, 152116.	2.8	20
122	Wear and Corrosion Performance of Al-Cu-Fe-(Cr) Quasicrystalline Coatings Produced by HVOF. Journal of Thermal Spray Technology, 2020, 29, 1195-1207.	1.6	20
123	Microstructure and mechanical properties of spray deposited and extruded/heat treated hypoeutectic Al–Si alloy. Materials Science & Engineering A: Structural Materials: Properties, Microstructure and Processing, 2007, 449-451, 850-853.	2.6	19
124	Laser remelting of Al91Fe4Cr3Ti2 quasicrystalline phase former alloy. Journal of Alloys and Compounds, 2010, 495, 646-649.	2.8	19
125	Microstructural characterization and hydrogenation study of extruded MgFe alloy. Journal of Alloys and Compounds, 2010, 504, S299-S301.	2.8	19
126	2Mg–Fe alloys processed by hot-extrusion: Influence of processing temperature and the presence of MgO and MgH2 on hydrogenation sorption properties. Journal of Alloys and Compounds, 2011, 509, S460-S463.	2.8	19

WALTER JOSé BOTTA

#	Article	IF	CITATIONS
127	Ordered phases and texture in spray-formed Fe–5wt%Si. Journal of Alloys and Compounds, 2011, 509, S260-S264.	2.8	19
128	Surface chemical treatment of ultrafine-grained Ti–6Al–7Nb alloy processed by severe plastic deformation. Journal of Alloys and Compounds, 2015, 643, S241-S245.	2.8	19
129	Mg-based Nanocomposites for Hydrogen Storage Containing Ti-Cr-V Alloys as Additives. Materials Research, 2016, 19, 80-85.	0.6	19
130	Low temperature rolling of AZ91 alloy for hydrogen storage. International Journal of Hydrogen Energy, 2017, 42, 29394-29405.	3.8	19
131	Predicting the Formation of Intermetallic Phases in the Al-Si-Fe System with Mn Additions. Journal of Phase Equilibria and Diffusion, 2017, 38, 298-304.	0.5	19
132	Improved ball milling method for the synthesis of nanocrystalline TiFe compound ready to absorb hydrogen. International Journal of Hydrogen Energy, 2020, 45, 2084-2093.	3.8	19
133	Mechanical multiple relaxation spectra in Nbî—,Zeî—,O alloys. Acta Metallurgica Et Materialia, 1990, 38, 391-396.	1.9	18
134	Thermodynamic predictions for the formation of ceramic-metal composite by self-propagating high-temperature synthesis. Journal of Materials Science Letters, 1991, 10, 819-823.	0.5	18
135	Synthesis of Al2O3–NbC by reactive milling and production of nanocomposites. Journal of Materials Processing Technology, 2003, 143-144, 185-190.	3.1	18
136	Outâ€ofâ€Plane Magnetic Patterning Based on Indentationâ€Induced Nanocrystallization of a Metallic Glass. Small, 2010, 6, 1543-1549.	5.2	18
137	Microstructure and mechanical properties of Al–Si–Mg ribbons. Journal of Alloys and Compounds, 2010, 495, 386-390.	2.8	18
138	Magnesium-Nickel alloy for hydrogen storage produced by melt spinning followed by cold rolling. Materials Research, 2012, 15, 813-817.	0.6	18
139	Hydrogen storage properties of MgH2 processed by cold forging. Journal of Alloys and Compounds, 2014, 615, S719-S724.	2.8	18
140	Characterization and Corrosion Resistance of Boron-Containing-Austenitic Stainless Steels Produced by Rapid Solidification Techniques. Materials, 2018, 11, 2189.	1.3	18
141	Changing the solidification sequence and the morphology of iron-containing intermetallic phases in AA6061 aluminum alloy processed by spray forming. Materials Characterization, 2018, 145, 507-515.	1.9	18
142	Effects of friction stir processing on hydrogen storage of ZK60 alloy. International Journal of Hydrogen Energy, 2018, 43, 11085-11091.	3.8	18
143	Influence of chromium concentration and partial crystallization on the corrosion resistance of FeCrNiB amorphous alloys. Materials Characterization, 2021, 179, 111369.	1.9	18
144	FeNiB-based metallic glasses with fcc crystallisation products. Journal of Non-Crystalline Solids, 2002, 304, 44-50.	1.5	17

#	Article	IF	CITATIONS
145	Crystallisation behaviour and glass-forming ability in Al–La–Ni system. Journal of Alloys and Compounds, 2010, 495, 334-337.	2.8	17
146	Structural characterization and hydrogen storage properties of MgH 2 –Mg 2 CoH 5 nanocomposites. International Journal of Hydrogen Energy, 2017, 42, 14593-14601.	3.8	17
147	Formation and stability of complex metallic phases including quasicrystals explored through combinatorial methods. Scientific Reports, 2019, 9, 7136.	1.6	17
148	Glass transition Tg, thermal expansion, and quenched-in free volume ΔVf in pyrex glass measured by time-resolved X-ray diffraction. Journal of Alloys and Compounds, 2005, 388, L1-L3.	2.8	16
149	Design and production of Al-Mn-Ce alloys with tailored properties. Materials and Design, 2016, 110, 436-448.	3.3	16
150	Effect of Cr addition on the formation of the decagonal quasicrystalline phase of a rapidly solidified Al-Ni-Co alloy. Journal of Alloys and Compounds, 2017, 707, 41-45.	2.8	16
151	Processing of MgH2 by extensive cold rolling under protective atmosphere. International Journal of Hydrogen Energy, 2017, 42, 2201-2208.	3.8	16
152	Tailoring the microstructure of recycled 319 aluminum alloy aiming at high ductility. Journal of Materials Research and Technology, 2019, 8, 3539-3549.	2.6	16
153	Formation of Metallic Glass Coatings by Detonation Spraying of a Fe66Cr10Nb5B19 Powder. Metals, 2019, 9, 846.	1.0	16
154	Metastable phases, quasicrystals and solid solutions in Zr-based bulk glass-forming alloys. Scripta Materialia, 2001, 44, 1239-1244.	2.6	15
155	Hydrogen Activation Behavior of Commercial Magnesium Processed by Different Severe Plastic Deformation Routes. Materials Science Forum, 2010, 667-669, 1047-1051.	0.3	15
156	Microstructural characterization of Ti-6Al-7Nb alloy after severe plastic deformation. Materials Research, 2012, 15, 786-791.	0.6	15
157	Assessing technological developments in amorphous/glassy metallic alloys using patent indicators. Journal of Alloys and Compounds, 2017, 716, 330-335.	2.8	15
158	Effect of iron on the microstructure and mechanical properties of the spray-formed and rotary-swaged 319 aluminum alloy. International Journal of Advanced Manufacturing Technology, 2019, 102, 3879-3894.	1.5	15
159	Designing new quasicrystalline compositions in Al-based alloys. Journal of Alloys and Compounds, 2020, 823, 153765.	2.8	15
160	Formation, thermal stability and mechanical properties of high-entropy (Fe0.25Co0.25Ni0.25Cr0.125Mo0.0625Nb0.0625)100‒Bx (xÂ= 7–14) amorphous alloys. Journal of Alloys ar Compounds, 2020, 825, 153858.	nd2.8	15
161	Microstructure and wear resistance of spray-formed supermartensitic stainless steel. Materials Research, 2013, 16, 642-646.	0.6	15
162	Heat treatment of amorphous Al90Fe5Nd5 and Al88FeNi6Nd5 alloys. Journal of Non-Crystalline Solids, 2000, 273, 266-270.	1.5	14

#	Article	IF	CITATIONS
163	Electromechanical shaping, assembly and engraving of bulk metallic glasses. Materials Science & Engineering A: Structural Materials: Properties, Microstructure and Processing, 2004, 375-377, 227-234.	2.6	14
164	Spray forming of the glass former Fe83Zr3.5Nb3.5B9Cu1 alloy. Materials Science & Engineering A: Structural Materials: Properties, Microstructure and Processing, 2004, 375-377, 571-576.	2.6	14
165	High-Yield Direct Synthesis of Mg <sub>2</sub> FeH <sub>6</sub> from the Elements by Reactive Milling. Solid State Phenomena, 2011, 170, 259-262.	0.3	14
166	Nanostructured MgH2 obtained by cold rolling combined with short-time high-energy ball milling. Materials Research, 2013, 16, 158-163.	0.6	14
167	The role of yttrium and oxygen on the crystallization behavior of a Cu–Zr–Al metallic glass. Journal of Non-Crystalline Solids, 2014, 406, 79-87.	1.5	14
168	Hydrogen storage properties of 2Mg–Fe after the combined processes of hot extrusion and cold rolling. Journal of Alloys and Compounds, 2014, 586, S409-S412.	2.8	14
169	Insight into the complex ternary phase behavior in Al-Mn-Ce alloys. Journal of Alloys and Compounds, 2017, 727, 460-468.	2.8	14
170	Wear Resistant Duplex Stainless Steels Produced by Spray Forming. Metals and Materials International, 2019, 25, 456-464.	1.8	14
171	Corrosion resistant and tough multi-principal element Cr-Co-Ni alloys. Journal of Alloys and Compounds, 2021, 884, 161107.	2.8	14
172	Glass transition, thermal expansion and relaxation in B2O3 glass measured by time-resolved X-ray diffraction. Journal of Non-Crystalline Solids, 2008, 354, 325-327.	1.5	13
173	Mechanical behavior under nanoindentation of a new Ni-based glassy alloy produced by melt-spinning and copper mold casting. Journal of Non-Crystalline Solids, 2010, 356, 2251-2257.	1.5	13
174	Amorphous phase formation by spray forming of alloys [(Fe0.6Co0.4)0.75B0.2Si0.05]96Nb4 and Fe66B30Nb4 modified with Ti. Journal of Alloys and Compounds, 2011, 509, S148-S154.	2.8	13
175	Controlled mechanochemical synthesis and hydrogen desorption mechanisms of nanostructured Mg2CoH5. International Journal of Hydrogen Energy, 2015, 40, 1504-1515.	3.8	13
176	Microstructure formation and abrasive wear resistance of a boron-modified superduplex stainless steel produced by spray forming. Journal of Materials Research, 2016, 31, 2987-2993.	1.2	13
177	Synthesis of Nanostructured TiFe Hydrogen Storage Material by Mechanical Alloying via Highâ€Pressure Torsion. Advanced Engineering Materials, 2020, 22, 2000011.	1.6	13
178	In-situ crystallization of amorphous Fe73â^'xNbxAl4Si3B20 alloys through synchrotron radiation. Journal of Non-Crystalline Solids, 2006, 352, 3404-3409.	1.5	12
179	Selection of good glass former compositions in Ni–Ti system using a combination of topological instability and thermodynamic criteria. Journal of Non-Crystalline Solids, 2008, 354, 1932-1935.	1.5	12
180	Mechanochemistry and H-sorption properties of Mg2FeH6-based nanocomposites. International Journal of Materials Research, 2012, 103, 1147-1154.	0.1	12

#	Article	IF	CITATIONS
181	Electrochemical Corrosion Behavior of Spray-Formed Boron-Modified Supermartensitic Stainless Steel. Metallurgical and Materials Transactions A: Physical Metallurgy and Materials Science, 2017, 48, 2077-2089.	1.1	12
182	Effects of graphite addition and air exposure on ball-milled Mg–Al alloys for hydrogen storage. International Journal of Hydrogen Energy, 2019, 44, 23257-23266.	3.8	12
183	Wear Resistance of Boron-Modified Supermartensitic Stainless Steel Coatings Produced by High-Velocity Oxygen Fuel Process. Journal of Thermal Spray Technology, 2019, 28, 2003-2014.	1.6	12
184	Phase separation and nanocrystallization in Al92Sm8metallic glass. Philosophical Magazine, 2006, 86, 4235-4242.	0.7	11
185	Microstructure and mechanical properties of spray co-deposited Al–8.9wt.% Si–3.2wt.% Cu–0.9wt.% Fe+(Al–3wt.% Mn–4wt.% Si)p composite. Journal of Alloys and Compounds, 2007, 434-435, 371-374.	2.8	11
186	Thermodynamic and topological instability approaches for forecasting glass-forming ability in the ternary Al–Ni–Y system. Journal of Alloys and Compounds, 2008, 464, 118-121.	2.8	11
187	Prediction of good glass formers in the Al-Ni-La and Al-Ni-Gd systems using topological instability and electronegativity. Journal of Applied Physics, 2011, 109, .	1.1	11
188	Nanoporous titanium obtained from a spinodally decomposed Ti alloy. Microporous and Mesoporous Materials, 2016, 222, 23-26.	2.2	11
189	FCC phase formation in immiscible Mg–Hf (magnesium–hafnium) system by high-pressure torsion. AlP Advances, 2020, 10, .	0.6	11
190	Hydrogen absorption/desorption reactions of the (TiVNb)85Cr15 multicomponent alloy. Journal of Alloys and Compounds, 2022, 901, 163620.	2.8	11
191	Directional and rapid solidification of Al–Nb–Ni ternary eutectic alloy. Materials Science & Engineering A: Structural Materials: Properties, Microstructure and Processing, 2004, 375-377, 565-570.	2.6	10
192	Rapidly solidified Al92Fe3Cr2Mn3 alloy. Materials Science & Engineering A: Structural Materials: Properties, Microstructure and Processing, 2007, 449-451, 1057-1061.	2.6	10
193	Evaluation of glass forming ability in the Ni–Nb–Zr alloy system by the topological instability (λ) criterion. Journal of Alloys and Compounds, 2010, 495, 313-315.	2.8	10
194	Class formation of alloys selected by lambda and electronegativity criteria in the Ti–Zr–Fe–Co system. Journal of Alloys and Compounds, 2010, 495, 316-318.	2.8	10
195	Formation reaction of Mg2FeH6: effect of hydrogen absorption/desorption kinetics. Materials Research, 2013, 16, 1373-1378.	0.6	10
196	Residual glass and crystalline phases in a barium disilicate glass–ceramic. Materials Characterization, 2015, 110, 192-196.	1.9	10
197	Effect of dislocations and residual stresses on the martensitic transformation of Cu-Al-Ni-Mn shape memory alloy powders. Journal of Alloys and Compounds, 2017, 723, 841-849.	2.8	10
198	Synthesis, characterization and first hydrogen absorption/desorption of the Mg35Al15Ti25V10Zn15 high entropy alloy. International Journal of Hydrogen Energy, 2022, 47, 22881-22892.	3.8	10

#	Article	IF	CITATIONS
199	Solution hardening and softening of Nb-Zr single crystals. Philosophical Magazine A: Physics of Condensed Matter, Structure, Defects and Mechanical Properties, 1988, 57, 703-716.	0.8	9
200	Microstructures and mechanical properties of bulk AlFeNd(Cu,Si) alloys obtained through centrifugal force casting. Materials Science & Engineering A: Structural Materials: Properties, Microstructure and Processing, 2007, 452-453, 161-169.	2.6	9
201	Hot Extrusion of Nanostructured Al-Powder Alloys: Grain Growth Control and the Effect of Process Parameters on Their Microstructure and Mechanical Properties. Metallurgical and Materials Transactions A: Physical Metallurgy and Materials Science, 2009, 40, 3314-3321.	1.1	9
202	Processing of glass former alloys by spray forming. Materialwissenschaft Und Werkstofftechnik, 2010, 41, 513-523.	0.5	9
203	Topological instability and glass forming ability of Al–Ni–Sm alloys. Journal of Alloys and Compounds, 2011, 509, S141-S144.	2.8	9
204	Hydrogen storage properties of 2Mg–Fe mixtures processed by hot extrusion: Influence of the extrusion ratio. International Journal of Hydrogen Energy, 2012, 37, 15196-15203.	3.8	9
205	Development of Ultrafine-Grained Metals by Equal-Channel Angular Pressing. , 2014, , 187-209.		9
206	Mechanical spectroscopy study on the Cu54Zr40Al6 amorphous matrix alloy at low temperature. Journal of Alloys and Compounds, 2015, 621, 319-323.	2.8	9
207	Ultrafine-Grained Ti-13Nb-13Zr Alloy Produced by Severe Plastic Deformation. Materials Research, 2017, 20, 404-410.	0.6	9
208	Microstructure and mechanical behavior of Al92Fe3Cr2X3 (X = Ce, Mn, Ti, and V) alloys processed by centrifugal force casting. Journal of Materials Research and Technology, 2019, 8, 2092-2097.	2.6	9
209	Functionally graded aluminum reinforced with quasicrystal approximant phases – Improving the wear resistance at high temperatures. Wear, 2020, 462-463, 203507.	1.5	9
210	The influence of the O2/C2H2 ratio on the structure and properties of Fe66Cr10Nb5B19 detonation coatings. Materials Today: Proceedings, 2020, 25, 384-386.	0.9	9
211	Strong and ductile recycled Al-7Si-3Cu-1Fe alloy: Controlling the morphology of quasicrystal approximant α-phase by Mn and V addition. Journal of Alloys and Compounds, 2021, 888, 161508.	2.8	9
212	Hydrogen Absorption/Desorption Behavior of a Cold-Rolled TiFe Intermetallic Compound. Materials Research, 2021, 24, .	0.6	9
213	Rapid solidification of an Al-5Ni alloy processed by spray forming. Materials Research, 2012, 15, 779-785.	0.6	8
214	Microstructural evolution of Ti-6Al-7Nb alloy during high pressure torsion. Materials Research, 2012, 15, 792-795.	0.6	8
215	Microstructure of a recycled AA7050 alloy processed by spray forming followed by hot extrusion and rotary swaging. Materialwissenschaft Und Werkstofftechnik, 2014, 45, 568-573.	0.5	8
216	Thermodynamic Calculations for the Investigation of Phase Formation in Boron-Modified Ferritic Stainless Steel. Journal of Phase Equilibria and Diffusion, 2017, 38, 343-349.	0.5	8

#	Article	IF	CITATIONS
217	Synthesis of β-Ti-Nb alloys from elemental powders by high-energy ball milling and their hydrogenation features. International Journal of Hydrogen Energy, 2018, 43, 18382-18391.	3.8	8
218	Outstanding Tensile Ductility in High Iron-Containing Al-Si-Cu Alloys. Metallurgical and Materials Transactions A: Physical Metallurgy and Materials Science, 2020, 51, 2703-2710.	1.1	8
219	Severe Plastic Deformation and Additive Distribution in Mg-Fe to Improve Hydrogen Storage Properties. Materials Research, 2017, 20, 61-70.	0.6	8
220	Electromechanical engraving and writing on bulk metallic glasses. Applied Physics Letters, 2002, 81, 1606-1608.	1.5	7
221	Extrusion of nanocomposite Al90Fe5Nd5 powders and characterization of the consolidated material. Materials Science & Engineering A: Structural Materials: Properties, Microstructure and Processing, 2003, 344, 57-63.	2.6	7
222	Effect of interstitial impurities on internal friction measurements in niobium. Materials Science & Engineering A: Structural Materials: Properties, Microstructure and Processing, 2004, 370, 131-134.	2.6	7
223	Correlation between heat- and deformation-induced crystallization of amorphous Al alloys. Philosophical Magazine Letters, 2008, 88, 863-870.	0.5	7
224	2Mg–Fe and 2Mg–Fe+5%C mixtures processed by hot extrusion: Influence of carbon on hydrogen sorption properties. Journal of Alloys and Compounds, 2011, 509, S464-S467.	2.8	7
225	Microstructural characterization of high-silicon iron alloys produced by spray forming and co-injection of Si particles. Journal of Alloys and Compounds, 2011, 509, S254-S259.	2.8	7
226	Characterization of Glass Forming Alloy Fe <sub>43.2</sub> Co <sub>28.8</sub> B <sub>19.2</sub> Si <sub>4.8</sub> Nb <sub>4</sub> Processed by Spray Forming and Wedge Mold Casting Techniques. Materials Science Forum, 2011, 691, 23-26.	0.3	7
227	Mg2FeH6-based nanocomposites with high capacity of hydrogen storage processed by reactive milling. Materials Research, 2012, 15, 229-235.	0.6	7
228	Comparative study of nanoindentation on melt-spun ribbon and bulk metallic glass with Ni60Nb37B3 composition. Journal of Materials Research, 2013, 28, 2740-2746.	1.2	7
229	Hydrogen storage properties of 2Mg-Fe mixtures processed by hot extrusion at different temperatures. International Journal of Hydrogen Energy, 2017, 42, 11493-11500.	3.8	7
230	Hydrogen desorption/absorption properties of the extensively cold rolled β Ti–40Nb alloy. International Journal of Hydrogen Energy, 2019, 44, 20133-20144.	3.8	7
231	Hydrogen storage properties of filings of the ZK60 alloy modified with 2.5Âwt% mischmetal. International Journal of Hydrogen Energy, 2020, 45, 5375-5383.	3.8	7
232	Formation, structure and properties of pseudo-high entropy clustered bulk metallic glasses. Journal of Alloys and Compounds, 2020, 820, 153164.	2.8	7
233	Room temperature conversion of Mg to MgH2 assisted by low fractions of additives. International Journal of Hydrogen Energy, 2022, 47, 470-489.	3.8	7
234	Shaping of Bulk Metallic Glasses by Simultaneous Application of Electrical Current and Low Stress. Materials Research Society Symposia Proceedings, 2000, 644, 12201.	0.1	6

#	Article	IF	CITATIONS
235	Predicting glass-forming compositions in the Al–La and Al–La–Ni systems. Journal of Alloys and Compounds, 2011, 509, S170-S174.	2.8	6
236	Strengthening Mechanisms of 27MnSiVS6 Microalloyed Steel Deformed by Four Different Forging Processes. Procedia Engineering, 2011, 10, 512-517.	1.2	6
237	Reactive Milling of Magnesium under Hydrogen Using Transition Metals and their Fluorides as Additives. Solid State Phenomena, 0, 194, 232-236.	0.3	6
238	A synchrotron X-ray diffraction study of hydrogen storage and enhanced sorption kinetics in a mini-tank of Mg with crystalline and amorphous catalytic particle additions. Journal of Alloys and Compounds, 2012, 540, 57-61.	2.8	6
239	Comparative study between two die cast methods for processing Cu–Zr–Al bulk metallic glasses. Journal of Materials Research and Technology, 2013, 2, 125-129.	2.6	6
240	Synthesis by High-Energy Ball Milling of MgH <sub>2</sub> -TiFe Composites for Hydrogen Storage. Materials Science Forum, 0, 899, 13-18.	0.3	6
241	An Overview of Thermally Sprayed Fe-Cr-Nb-B Metallic Glass Coatings: From the Alloy Development to the Coating's Performance Against Corrosion and Wear. Journal of Thermal Spray Technology, 2022, 31, 923-955.	1.6	6
242	Structure and orientation of zirconia in a niobium metal matrix. Acta Metallurgica, 1985, 33, 477-486.	2.1	5
243	The deformation of Nb–N single crystals at low temperatures. Philosophical Magazine A: Physics of Condensed Matter, Structure, Defects and Mechanical Properties, 1989, 60, 205-225.	0.8	5
244	Effect of Dislocation Mechanisms during Extrusion of Nanostructured Aluminum Powder Alloy. Metallurgical and Materials Transactions A: Physical Metallurgy and Materials Science, 2009, 40, 3322-3330.	1.1	5
245	Formation and microstructure of Ni62- x Nb38Ti x (x = 3, 6, 10 at.%) bulk metallic glasses. International Journal of Materials Research, 2012, 103, 1096-1101.	0.1	5
246	Corrosion resistance and glass forming ability of Fe47Co7Cr15M9Si5B15Y2 (M=Mo, Nb) amorphous alloys. Materials Research, 2013, 16, 1294-1298.	0.6	5
247	Exploring several different routes to produce Mg- based nanomaterials for Hydrogen storage. IOP Conference Series: Materials Science and Engineering, 2014, 63, 012115.	0.3	5
248	Assessment of phase constitution on the Al-rich region of rapidly solidified Al-Co-Fe-Cr alloys. Materials Characterization, 2016, 122, 76-82.	1.9	5
249	Investigation by mechanical spectroscopy at different frequencies of the nucleation processes in amorphous Cu-Zr-Al alloys. Materials Science & Engineering A: Structural Materials: Properties, Microstructure and Processing, 2017, 694, 66-71.	2.6	5
250	Magnesium Alloys for Hydrogen Storage Processed by ECAP Followed by Low Temperature Rolling. Materials Research, 0, 25, .	0.6	5
251	Microstructural characterization of spray formed Fe66B30Nb4 alloy. Journal of Alloys and Compounds, 2010, 495, 417-419.	2.8	4
252	Mechanical spectroscopy study of the Cu36Zr59Al5 and Cu54Zr40Al6 amorphous alloys. Materials Research, 2012, 15, 1070-1074.	0.6	4

#	Article	IF	CITATIONS
253	The effect of oxygen on the microstructural evolution in crystallized Cu–Zr–Al metallic glasses. Intermetallics, 2015, 65, 51-55.	1.8	4
254	Experimental and thermodynamic investigation of the microstructural evolution of a boron-rich Fe-Cr-Nb-B alloy. Journal of Alloys and Compounds, 2017, 713, 119-124.	2.8	4
255	Study of Glass Forming on Cu60.0Zr32.5Ti7.5 Alloy by Molecular Dynamics Simulation. Materials Research, 2018, 21, .	0.6	4
256	A ceramic matrix composite obtained by highly exothermic reaction. Journal of the European Ceramic Society, 1992, 9, 67-73.	2.8	3
257	Anelastic relaxation due to Oî—,H pairs in Nbî—,Zr alloys. Journal of Alloys and Compounds, 1994, 211-212, 226-228.	2.8	3
258	On the B2 → fcc transformation of Fe–Rh during deformation. Philosophical Magazine A: Physics of Condensed Matter, Structure, Defects and Mechanical Properties, 2000, 80, 1779-1793.	0.8	3
259	Consolidation of Mechanically Alloyed Aluminium Matrix Composite Powders by Severe Plastic Deformation. Journal of Metastable and Nanocrystalline Materials, 2003, 15-16, 307-312.	0.1	3
260	Hydrogen Sorption Properties of the Complex Hydride Mg <sub>2</sub> FeH <sub>6</sub> Consolidated by HPT. Materials Science Forum, 2010, 667-669, 1053-1058.	0.3	3
261	Diffusion of Interstitial Solutes in Nb-46wt% Ti Alloys Measured by Mechanical Spectroscopy. Defect and Diffusion Forum, 2012, 326-328, 708-712.	0.4	3
262	Overspray Powder Characterization of Fe-Based Glassy Alloy. Materials Science Forum, 0, 727-728, 468-475.	0.3	3
263	Atomic structure of bulk metallic glasses and their supercooled liquid states probed by high-energy synchrotron light. Comptes Rendus Physique, 2012, 13, 218-226.	0.3	3
264	Microstructure evolution of AA7050 Al alloy during Equal-Channel Angular Pressing. Materials Research, 2012, 15, 732-738.	0.6	3
265	Influence of Al Additions on the Microstructure and Mechanical Properties of a C and Si-Free High-Mn Steel. Metals, 2020, 10, 352.	1.0	3
266	Phase decomposition and mechanical properties of pseudo-high entropy Zr65(Al,Fe,Co,Ni,M)35 (M=Cu,) Tj ETQq(	0 0 0 rgBT 2.8 rgBT	/gverlock 10
267	Hot Consolidation of Partially Amorphous Cu-Ti Based Alloy: a Comparison Between Hot Extrusion and Hot Compaction by Sintering. Materials Research, 2015, 18, 448-452.	0.6	3
268	A wear-resistant Al85Cu6Fe3Cr6 spray-formed quasicrystalline composite. Materialia, 2022, 21, 101367.	1.3	3
269	Microstructural Characterization of Spray Formed Al <sub>72</sub> Si <sub>14</sub> Fe <sub>14</sub> Alloy. Journal of Metastable and Nanocrystalline Materials, 2004, 20-21, 659-664.	0.1	2
270	Influence of the atomization gas on the microstructure and magnetic properties of spray-formed Fe–3%Si–3.5%Al alloys. Materials Science & Engineering A: Structural Materials: Properties, Microstructure and Processing, 2008, 477, 9-14.	2.6	2

#	Article	IF	CITATIONS
271	Selection of new glass-forming compositions in Al–La system using a combination of topological instability and thermodynamic criteria. Materials Science & Engineering A: Structural Materials: Properties, Microstructure and Processing, 2009, 512, 53-57.	2.6	2
272	2Mg-Fe Alloy Processed by Hot Extrusion: Influence of Particle Size and Extrusion Reduction Ratio on Hydrogenation Properties. Materials Science Forum, 0, 691, 3-9.	0.3	2
273	Anelastic Relaxation Measurements in Nb-46wt%Ti Alloys with Interstitial Solutes in Solid Solution. Solid State Phenomena, 2012, 184, 92-97.	0.3	2
274	Stability of an amorphous alloy of the Mm-Al-Ni-Cu system. Materials Research, 2012, 15, 757-762.	0.6	2
275	Processing and microstructural characterization of a Ti-Cr-Nb alloy synthesized by high-energy ball-milling. Materials Research, 2012, 15, 753-756.	0.6	2
276	Consolidation of the Cu46Zr42Al7Y5 amorphous ribbons and powder alloy by hot extrusion. Materials Research, 2012, 15, 728-738.	0.6	2
277	On the ternary eutectic reaction in the Fe 60 Cr 8 Nb 8 B 24 quaternary alloy. Journal of Alloys and Compounds, 2017, 707, 281-286.	2.8	2
278	Assessing Collaboration and Knowledge Flow on Coatings of Metallic Glasses Obtained From Thermal Spraying Processes Using Bibliometrics and Science Mapping. Materials Research, 2017, 20, 71-80.	0.6	2
279	Thermal Spraying Processes and Amorphous Alloys: Macro-Indicators of Patent Activity. Materials Research, 2017, 20, 89-95.	0.6	2
280	Hydrogen storage properties of 2ÂMg–Fe mixtures processed by hot extrusion: Effect of ram speeds. International Journal of Hydrogen Energy, 2019, 44, 20203-20212.	3.8	2
281	Compositional influence on heating-induced clustered glass formation for multicomponent Zr55-60Al10(Co,Ni,Cu,Ag)30-35 alloys. Intermetallics, 2021, 135, 107233.	1.8	2
282	Microstructure Characterization and Kinetics of Crystallization Behavior of Tubular Spray Formed Fe43.2Co28.8B19.2Si4.8Nb4 Bulk Metallic Glass*. HTM - Journal of Heat Treatment and Materials, 2014, 69, 312-321.	0.1	2
283	Structural transformations of a gas-atomized Al62.5Cu25Fe12.5 alloy during detonation spraying, spark plasma sintering and hot pressing. Science of Sintering, 2021, 53, 379-386.	0.5	2
284	The deformation of a model metal-ceramic material; Nb-ZrO2single crystals. Philosophical Magazine A: Physics of Condensed Matter, Structure, Defects and Mechanical Properties, 1989, 59, 603-628.	0.8	1
285	The deformation of a model metal-ceramic material: Nb-ZrO2single crystals. Philosophical Magazine A: Physics of Condensed Matter, Structure, Defects and Mechanical Properties, 1989, 59, 581-601.	0.8	1
286	Consolidation of Easy Glass Former Zr <sub>55</sub> Cu <sub>30</sub> Al <sub>10</sub> Ni <sub>5</sub> Alloy Ribbons by Severe Plastic Deformation. Journal of Metastable and Nanocrystalline Materials, 2004, 20-21, 253-256.	0.1	1
287	Structural Comparison of Amorphous, Nanocrystalline and Microcrystalline Al <sub>90</sub> Fe <sub>7</sub> Nb <sub>3</sub> Alloys. Materials Science Forum, 0, 727-728, 3-8.	0.3	1
288	New Zr-based glass-forming alloys containing Gd and Sm. Materials Research, 2012, 15, 723-727.	0.6	1

#	Article	IF	CITATIONS
289	Corrosion Resistant Boron-Modified Ferritic and Austenitic Stainless Steels Designed by CALPHAD. Metallurgical and Materials Transactions A: Physical Metallurgy and Materials Science, 2021, 52, 2708-2719.	1.1	1
290	Pitting Resistance of Al90Fe7Nb3 and Al90Fe7Zr3 Nanocrystalline Alloys Obtained by Melt-Spinning and Hot Extrusion. Portugaliae Electrochimica Acta, 2009, 27, 309-316.	0.4	1
291	Recent developments on fabrication of Al-matrix composites reinforced with quasicrystals: From metastable to conventional processing. Journal of Materials Research, 2021, 36, 1-17.	1.2	1
292	A model for rotation toughening in a crystal with diamond structure. Computational Materials Science, 1996, 6, 77-80.	1.4	0
293	Effects of the addition of SiC on the crystallization of Al84Ni8Co4Y3Zr1 (at.%) amorphous ribbons. Journal of Non-Crystalline Solids, 2008, 354, 4878-4882.	1.5	0
294	Effect of the addition of Mn on the tensile properties of a spray-formed and extruded Al-9Si-4Cu-1Fe alloy. Journal of Physics: Conference Series, 2009, 144, 012114.	0.3	0
295	Mechanical Spectroscopy Study on Cu <sub>53.5</sub> Zr <sub>42</sub> Al <sub>4.5</sub> Alloy. Defect and Diffusion Forum, 2011, 312-315, 1233-1237.	0.4	0
296	Selection of compositions with high glass forming ability in the Ni-Nb-B alloy system. Materials Research, 2012, 15, 718-722.	0.6	0
297	Study on Cu <sub>48</sub> Zr <sub>43</sub> Al <sub>9</sub> and Cu <sub>54</sub> Zr <sub>40</sub> Al <sub>6</sub> Amorphous Matrix Alloys by Mechanical Spectroscopy. Defect and Diffusion Forum, 2015, 365, 317-322.	0.4	0
298	Characterization of Atomized Powders and Extruded Samples of an Al-Si-Cu Alloy. Materials Science Forum, 0, 899, 442-447.	0.3	0
299	Micro-structural characterization of supermartensitic stainless steel coating modified with boro processed by HVOF. Microscopy and Microanalysis, 2020, 26, 97-98.	0.2	0